LASER-DRIVEN PLASMA-CATHODE ELECTRON INJECTOR

D. Umstadter, S.-Y. Chen, E. Dodd, J.K. Kim, A. Maksimchuk and R. Wagner*
Center for Ultrafast Optical Science, University of Michigan, Ann Arbor, MI 48109

Abstract

We discuss the first experimental demonstration of electron acceleration by a laser wakefield over distances greater than a Rayleigh range (or the distance a laser normally propagates in vacuum). A self-modulated laser wakefield plasma wave is shown to have a field gradient that exceeds that of an RF linac by four orders of magnitude ($E \geq 200$ GV/m) and accelerates electrons with over 1-nC of charge per bunch in a beam with space-charge-limited emittance (1 mm-mrad). Above a laser power threshold, a plasma channel, created by the intense ultrashort laser pulse (I $\sim 4 \times 10^{18}$ W/cm^2, $\lambda = 1$ μm, τ=400 fs), was found to increase the laser propagation distance, decrease the electron beam divergence, and increase the electron energy. The plasma wave, directly measured with coherent Thomson scattering is shown to damp—due to beam loading—in a duration of 1.5 ps or $\sim$100 plasma periods We also discuss a new concept for controlled laser injection of electrons in order to create monoenergetic femtosecond electron bunches. As in the above experiments it uses the plasma itself as the cathode, but also an additional laser pulse as a trigger. By use of a 2-D particle-in-cell numerical code, it is shown that this technique will produce 1-femtosecond duration electron bunches with energy spread at the percent level.

1 INTRODUCTION

Due to recent advances in laser technology[1], it is now possible to generate the highest electromagnetic and electrostatic fields ever produced in the laboratory[2]. The interactions of these high-intensity and ultrashort-duration laser pulses with matter has come to be known as high-field science. In terms of basic research, these interactions permit for the first time the study of optics in relativistic plasmas. Technological applications include advanced fusion energy, x-ray lasers, and table-top ultrahigh-gradient electron accelerators. In the latter case, it may be possible to build an all-optical table-top injector, which produces GeV energy electron bunches with femtosecond pulse duration.

When an intense laser enters a region of gaseous-density atoms, the atomic electrons feel the enormous laser electromagnetic field, and begin to oscillate at the laser frequency ($\omega = 2\pi c/\lambda = ck$) . The oscillations can become so large that the electrons become stripped from the atoms, or ionized. At high laser intensity (I), the free electrons begin to move at close to the speed of light (c), and thus their mass m_e changes significantly compared to their rest mass. This large electron oscillation energy corresponds to gigabar laser pressure, displacing the electrons from regions of high laser intensity. Due to their much greater inertia, the ions remain stationary, providing an electrostatic restoring force. These effects cause the plasma electrons to oscillate at the plasma frequency (ω_p) after the laser pulse passes by them, creating alternating regions of net positive and negative charge, where $\omega_p = \sqrt{4\pi e^2 n_e/\gamma m_e}$, n_e is the electron density, e is the electron charge and γ is the relativistic factor associated with the electron motion transverse to the laser propagation. γ depends on the normalized vector potential, a_o, by $\gamma = \sqrt{1 + a_o^2}$, where $a_o = \gamma v_{os}/c = eE/m_o \omega c = 8.5 \times 10^{-10} \lambda[\mu\text{m}] I^{1/2}[\text{W/cm}^2]$. The resulting electrostatic wakefield plasma wave propagates at a phase velocity nearly equal to the speed of light and thus can continuously accelerate hot electrons[3]. Up to now, most experiments have been done in the self-modulated laser wakefield regime[4, 5, 6], where the laser pulse duration is much longer than the plasma period, $\tau >> \tau_p = 2\pi/\omega_p$. In this regime, the forward Raman scattering instability can grow; where an electromagnetic wave ($\omega_o, \boldsymbol{k_o}$) decays into a plasma wave ($\omega_p, \boldsymbol{k_p}$) and electromagnetic side-bands ($\omega_o \pm \omega_p, \boldsymbol{k_o} \pm \boldsymbol{k_p}$).

2 RECENT RESULTS

A small number of relativistic hot electrons were observed in inertial-confinement-fusion experiments with long-pulse duration large-building size lasers and solid-density targets. However, it was shown only recently that electrons can be accelerated by a plasma wave driven by intense ultrashort-duration table-top laser pulses (I $\sim 4 \times 10^{18}$ W/cm^2, $\lambda = 1$ μm, $\tau \sim 0.5$ ps) and gaseous-density targets [7, 8]. Under similar conditions, electrons were even observed to have an energies up to 44 MeV, with an energy spread of 100%[9]. Recently, we have shown that the accelerated electron beam appeared to be naturally-collimated with a low-divergence angle (less than ten degrees), and had over 1-nC of charge per bunch[10].

In this experiment, we used a Ti:sapphire-Nd:glass laser system based on chirped-pulse-amplification that produces 3 J, 400 fs pulses at 1.053 μm. The 43 mm diameter beam was focused with an f/4 off-axis parabolic mirror to $r_o = 8.5$ μm (1/e^2), corresponding to vacuum intensities exceeding 4×10^{18} W/cm^2. This pulse was focused onto a supersonic helium gas jet with a sharp gradient (250 μm) and a long flat-topped interaction region (75 μm). The

* We would like to thank M. Downer and P. LeBlanc for their collaboration on our Thomson scattering measurments. This work is sponsored by Department of Energy/Lawrence Livermore National Laboratory subcontract B307953 and the National Science Foundation Science and Technology Center contract PHY 8920108.

maximum density varies linearly with backing pressure up to the maximum backing pressure of 1000 PSI, and an underdense plasma at 3.6×10^{19} cm^{-3} is formed by the foot of the laser pulse tunnel-ionizing the gas. This plasma density corresponds to a critical power of P_c = 470 GW. A sharp gradient and long interaction region are found to be essential.

Moreover, as shown in Fig. 1, acceleration occured in this experiment[10] only when the laser power exceeded a certain critical value, P_c, the threshold for relativistic self-focusing. The total number of accelerated electrons

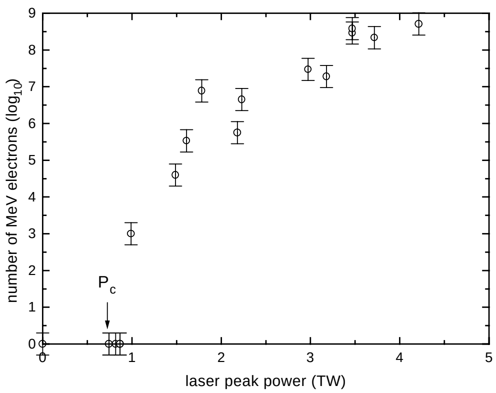

Figure 1: The number of relativistic electrons accelerated as a function of incident laser power focused in a gas of helium at atmospheric density.

(at all energies) was measured using either a Faraday cup or a plastic scintillator coupled to a photomultiplier tube, and the results were found to be consistent with each other. There is a sharp threshold for electron production at $\sim 1.5P_c$, and the total number of electrons increases exponentially and finally saturates beyond $4P_c$[10]. At $6P_c$, 6×10^9 accelerated electrons were measured coming out of the plasma in a beam. By using aluminum absorbers, we determined that 50% of the electrons detected have energy greater than 1 MeV (corresponding to 0.5 mJ of energy in the electron beam).

The electron energy spectrum (see Fig. 2) was measured using a 60° sector dipole magnet by imaging a LANEX scintillating screen with a CCD camera. The normalized distribution is found to have a functional form of exp$(-\alpha\gamma)$ where α is a fitting parameter. In the low power case ($< 6P_c$, no channeling), the normalized distribution follows exp$(-\gamma)$, and when the laser power increases ($> 6P_c$, with channeling), the electron energy distribution discretely jumps to follow exp(-0.67 γ). The abrupt change in the electron distribution also occurs if the laser power is held fixed and the density is increased, as it should given the critical power threshold dependence on density. Below 850 PSI (3.1×10^{19} cm^{-3}, no channeling), the electron distribution follows the same trend as the lower power distribution, and above 850 PSI (with channeling) it follows the higher power distribution. For the electron energy distribution greater than 3 MeV, a significantly less steep slope

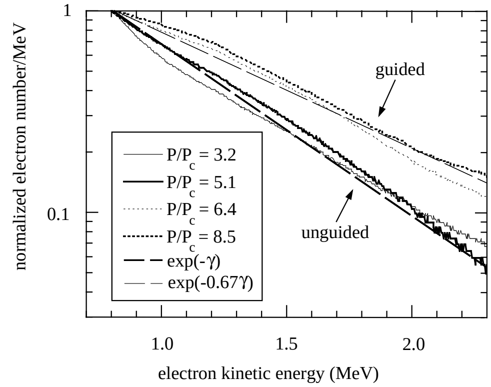

Figure 2: Normalized electron kinetic energy spectrum as a function of laser power at fixed electron density. The upper curves represent the spectra obtained when self-guiding was observed; the lower curves represent unguided spectra. The two exponential fits are also shown.

that extends to 20 MeV was measured using aluminum absorbers. Even though the plasma wave amplitude increases as the laser power increases, the distribution only dramatically changes when self-guiding occurs. This indicates that extension in the accelerating length is the primary factor in determining the fitting parameter α.

Measurements of the satellites in the spectrum of the forward scattered light indicated that a self-modulated plasma wave occurred when the laser power exceeded $P_c/2$. Since then, two independent research groups have simultaneously reported direct measurements of the plasma wave amplitude with a Thomson-scattering probe pulse[11, 12]. The field gradient was reported[12] to exceed that of a radio-frequency (RF) linac by four orders of magnitude ($E \geq$ 200 GV/m). This acceleration gradient corresponds to an energy gain of 1 MeV in a distance of only 10 microns. The plasma wave was observed to exist for a duration of 1.5 ps or 100 plasma oscillations[12]. It was calculated that it damps only because all of the wave energy was converted to the accelerated electrons. Except for the large energy spread and low average power, these parameters compare favorably with medical linacs. In fact, the much smaller source size of a laser wakefield accelerator compared with that of a conventional linac, 10 microns compared with greater than 100 microns, may permit much greater spatial resolution for medical imaging.

This enormous field gradient would be of limited use if the length over which it could be used to accelerate electrons were just the natural diffraction length of the highly focused laser beam, which is much less than a millimeter. Fortunately, we recently demonstrated that electrons can be accelerated beyond this distance[13]. At high laser power, the index of refraction in a plasma varies with the radius. This is both because the laser intensity varies with radius and the plasma frequency depends on the relativistic mass factor γ. Above the above-mentioned critical laser power P_c, the plasma should act like a positive lens and focus the laser beam, a process called relativistic self-focusing. This is similar to propagating a low power beam over an optical fiber optic cable, except in this case the intense laser makes its own fiber optic.

In order to diagnose the spatial extent of the plasma, a sidescattering imaging system with a spatial resolution of 15 μm was utilized. We were able to resolve the growth of the plasma channel as a function of both laser power and plasma density. Fig. 3 shows the sidescattered intensity distribution as a function of laser power, and the plasma channel clearly extends as the laser power increases. In the lower power cases ($< 2.6P_c$), the channel length is only ~ 125 μm, which is smaller than the confocal parameter ($2Z_R$) of 430 μm. As the laser power increases for a fixed gas density, the channel length first jumps to 250 μm at $3.9P_c$ and then reaches 750 μm at $7.2P_c$. The maximum channel length was observed to be 850 μm at $9.1P_c$. Note this is limited by the interaction length of the gas jet. At $5.5P_c$, the sidescattered image formed has two distinct foci, and when the power exceeds $7.2P_c$, either multiple foci or a channel are observed, depending on shot-to-shot fluctuations and the gas jet position. A similar channel extension occurs if the gas density is varied at fixed laser power. For a 3.9 TW laser pulse, the channel extends to 250 μm at 400 PSI backing pressure (1.4×10^{19} cm^{-3}, $3.2P_c$) and 750 μm at 800 PSI (2.9×10^{19} cm^{-3}, $7.0P_c$). The consistent behaviour at specific values of P_c for varying laser power or plasma density indicates that the channeling mechanism is relativistic self-focusing.

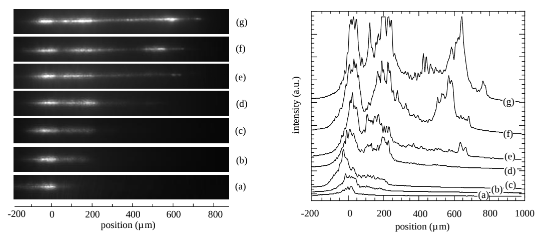

Figure 3: On-axis images (left) and corresponding lineouts (right) of sidescattered light at various laser powers and a fixed initial electron density of 3.6×10^{19} cm^{-3}. The various images and lineouts represent laser powers of $P/P_c =$ (a) 1.6, (b) 2.6, (c) 3.9, (d) 5.5, (e) 7.2, (f) 8.4, and (g) 9.1. Note: the curves have been displaced vertically for ease of viewing.

The sidescattered light was spectrally analyzed by an imaging spectrometer, and the bulk of the emission comes from incoherent Thomson scattering of the blue-shifted laser pulse. We were unable to obtain any information about the plasma density or temperature from this measurement. The divergence of the laser beam transmitted through the plasma was measured using a diffusing screen and a CCD camera with a 1.053 μm narrow bandpass filter. At all laser powers, the laser expands to twice the vacuum divergence, and we attribute this expansion to ionization defocusing. This is consistent with the strong blue-shifting we observe in the scattered spectra. Even though simulations indicate that the laser focuses to $\sim$2 μm[14], the complex dynamics that occur as the laser continually focuses and defocuses in the plasma make it impossible to determine the minimum self-focused beam width from the far field divergence angle.

A Maxwellian-like energy distribution has been observed in many previous experiments[15] and simulations[16], however no theoretical justification for it has been found to date. Because the energy distribution is exponential, a temperature in the longitudinal direction can be defined. The temperature of the low energy distribution changes from 500 keV (without guiding) to 750 keV (with guiding). In these plasmas, many different plasma waves can grow from various instabilities and local conditions. The interactions between these waves can lead to stochastic heating of the electron beam, so by extending the plasma length, the various waves will interact longer and heat the beam more. However, the dephasing length, $L_d = \lambda(\omega_o/\omega_p)^3$, which gives the maximum distance over which acceleration can occur (170 μm for our conditions), is significantly shorter than our accelerating length. From this expression, we would think that there would be no noticeable change in the electron spectrum when we extend the plasma length from 250 μm to 750 μm. Recent PIC simulations[16] indicate that this expression is too conservative for these highly nonlinear plasma interactions, and, in fact, the actual dephasing length may be many times longer. Consistent with our experimental results, these simulations indicate that the electron temperature, as well as the maximum energy, increase as the electrons propagate beyond the conventional dephasing length.

The relativistically self-guided channel was found to increase the laser propagation distance by a factor of four (limited thus far only by the length of gas), decrease the electron beam divergence by a factor of two (as shown in Fig. 4), and increase the electron energy. The electron beam profile was measured using a LANEX scintillating screen imaged by a CCD camera[10]. The LANEX is placed be-

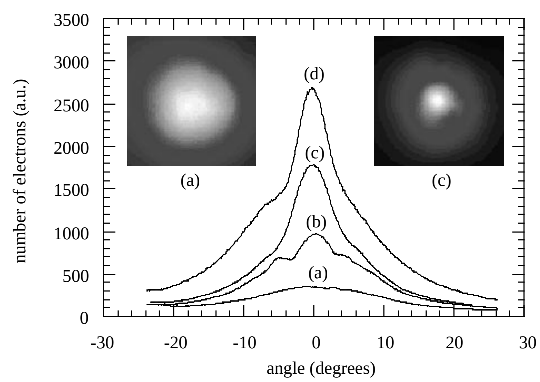

Figure 4: Electron beam divergence as a function of laser power. The various curves represent laser powers of $P/P_c =$ (a) 3.4, (b) 5.0, (c) 6.0, and (d) 7.5. The two insert figures show the complete beam images for curves (a) and (c).

hind an aluminum sheet which blocks the laser light, so only electrons greater than 100 keV can be imaged. Analysis of the electron spectrum indicates that the bulk of the electrons that create an image on the screen are in the 100 keV to 3 MeV range. We have found, using aluminum absorbers, that the electron divergence does not depend on electron energy in this range. At low power ($< 5P_c$), the electron beam has a Gaussian-like profile with a 10° radius at half-maximum (see Fig. 4). As the laser power increases and the plasma channel length increases to $\sim$250 μm, a second peak seems to grow out of the low-power profile. Ultimately at the highest laser powers and longest channel lengths, the divergence decreases to 5°, and the profile becomes more Lorentzian-like. The electron beam divergence should decrease as the longitudinal energy of the electrons increases since space charge will be less and the relative transverse momentum decreases due to the longer accelerating length. However, there should be a minimum divergence due to the space charge effect after the electrons leave the plasma. This effect is significant since the electrons are in the few MeV range (small γ) and the peak current is high (large number of electrons in a short bunch). We have roughly estimated the space charge divergence to be 6° by assuming 10^9 electrons at 1 MeV in a 1 ps bunch (note: $\theta_{hwhm} \propto \sqrt{N/\tau_e(\beta\gamma)^3}$, where N is the number of electrons, τ_e is the electron bunch duration, and $\beta\gamma$ is the normalized momentum of the electrons)[17]. The electron beam emittance can be found from the measured divergence angle and the radius of the plasma channel, and in the best case (5° half-angle and 5 μm half-max radius), the calculated emittance ($\epsilon = r_o\theta_{hwhm}$) is 0.4 π-mm-mrad. To verify that the reduction in the beam emittance is due to the extension of the plasma channel, another gas jet with a narrower width was used and the same measurements repeated. In this case, the sidescattered images show that the channel length is limited to 360 μm and the electron beam divergence is fixed at 12° for all laser powers.

3 FUTURE DIRECTIONS

In several recent papers[18], we proposed an alternative accelerator concept, which we call the resonant laser-plasma accelerator (RLPA), having the following advantages: (i) by utilizing a train of laser pulses with independently adjustable pulse widths and interpulse spacings, which are varied in an optimized manner, resonance with both the changing plasma-wave period and phase resonance width can be maintained in the nonlinear regime, and the maximum plasma-wave amplitude is achieved; (ii) lower plasma densities can be used, thus avoiding electron-phase detuning; and (iii) lower peak laser intensities can be used, thus allowing for a reduction of laser-plasma instabilities. We numerically determined the characteristics of the plasma wave generated by a nonevolving, optimized laser pulse train in 1-D. In Fig. 5(a), we plot the wake field resulting from single pulse excitation (LWFA) including fast oscillations of the laser pulse.

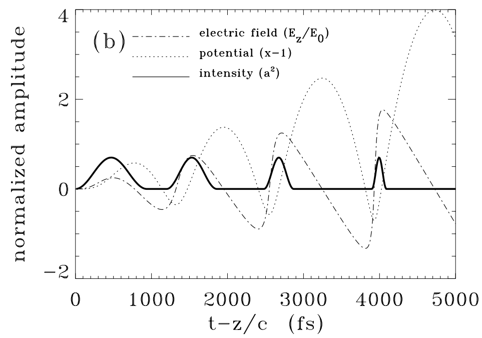

Figure 5: Numerical solutions for the RLPA with an optimized sine pulse train at $n_e = 10^{16}$ cm^{-3} with a_0 = 1.2.

In the above experiments, the plasma itself acted as the cathode (the source of the electrons). Since the electrons were picked up by the wave and accelerated with random phases, their energy spread was large. This may be acceptable for medical radiological sources, where broadband bremstrahlung x-ray radiation is created anyway, by focusing the electron beam onto a metal target. However, in order to create monoenergetic femtosecond duration electron bunches, a new concept for laser injection of electrons was also developed theorectically (as shown in Fig. 6), again using the plasma itself as the cathode but with laser triggering[19]. Either transverse (as shown), collinear or

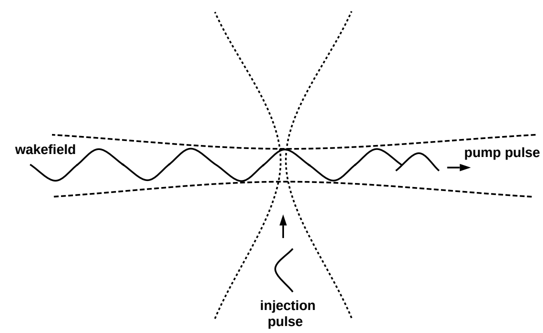

Figure 6: Schematic of the LILAC injector concept.

counter-propagating laser beams can be used for triggering. This is similar to giving several surfers identical pushes so that they all catch the same ocean wave in phase with one another. It was shown by use of a numerical code that with this method and by operating in the resonant wakefield regime ($\tau \sim \tau_p$), it should be possible to produce femtosecond electron bunches with energy spread at the percent level. We call the concept LILAC, which stands for Laser Injected Linear ACcelerator.

Normally, electrons oscillating in the plasma wave cannot be accelerated by the wake field since they are out of phase with it. Electrons that are not part of the plasma wave, however, can become trapped—i.e., continuously accelerated—by the plasma wave, provided that they are moving in the correct phase at nearly the phase velocity of the wave [20]. Since this velocity is close to the speed of light, it is generally thought that the required pre-acceleration can only be accomplished with a conventional linac. However, the low-field gradient (< 10 MeV/m) [17], of a first-stage conventional linac prolongs the time during which beam emittance can grow before the beam becomes relativistic; after this point, self-generated magnetic fields can balance the effects of space charge. Even with state-of-the-art electron guns, the pulsewidth of the electron bunch can be considerably longer than the plasma wave period of a second-stage laser-plasma accelerator. It will thus fill multiple acceleration buckets uniformly in phase space, resulting in a large energy spread. Also, it is difficult to position and focus the electron-beam in the plasma channel with micron accuracy, and synchronize the electron beam with the plasma wave acceleration phase. We have shown theoretically that it can simply be done with an additional laser pulse[19]. The basic idea is that once a laser wake field is excited by the longitudinal ponderomotive force of one laser pulse (the pump pulse), the transverse ponderomotive force of a second, orthogonally directed laser pulse (the injection pulse) can then be used to locally alter the trajectories of some of the plasma wave electrons such that they become in phase with the wave's electric field and thus accelerated to the trapping velocity[19].

By permitting the use of laser wake fields in the injection stage, this concept not only dispenses with the need to merge two dissimilar technologies, as in proposed hybrid systems[21], it also significantly increases the capabilities and applications of plasma-based accelerators. It is easier to synchronize in phase and overlap in space the processes of electron injection and acceleration by employing the same basic mechanism for both. Improved electron beam emittance may result from the increased field gradient in the first acceleration stage, by minimizing the time during which electrons are non-relativistic and thus most susceptible to space charge effects. A device based on this concept can be used either as a stand-alone accelerator system or as an injector for either conventional or plasma-based high-energy accelerators. Both the energetic electrons and the high-energy photons into which they can be converted have numerous industrial, medical and scientific applications.

As an injector stage for linear electron colliders for nuclear and high-energy physics, this pulse length reduction may have several interesting consequences. In the case of an electron-electron linear collider, it would have a higher limit on attainable luminosity by permitting a shorter β (in effect, the Rayleigh parameter of the magnetic optics) at the final focus/intersection point and it would also reduce beam-beam effects by reducing the time during which the beams overlap. There would also be a reduction in beam-beam Bremsstrahlung ("beamstrahlung") due to quantum mechanical effects. Such ultrashort-duration electron bunches may also become the basis for a new generation of table-top radiation sources. They may increase both the coherence and gain of synchrotrons, free-electron lasers, or Compton-scattering sources. Additionally, the ultrashort light-pulses that they may provide might be used to as "strobes" to probe temporal dynamics on the natural timescale of important ultrafast chemical, biological and physical processes.

4 REFERENCES

[1] P. Maine, D. Strickland, P. Bado, M. Pessot and G. Mourou, *IEEE J. Quantum Electron.* **QE-24**, 398 (1988).

[2] G. Mourou and D. Umstadter, *Phys. Fluids B* **4**, 2315 (1992).

[3] T. Tajima and J. M. Dawson, *Phys. Rev. Lett.* **43**, 267 (1979).

[4] N. E. Andreev, L. M. Gorbunov, V. I. Kirsanov, A. Pogosova and R. R. Ramazashvili, *Pis'ma Zh. Eksp. Teor. Fiz.*, **55** 551 (1992) [*JETP Lett.*, **55**, 571 (1992)].

[5] T. M. Antonsen, Jr., and P. Mora, *Phys. Rev. Lett.*, **69**, 2204 (1992).

[6] P. Sprangle, E. Esarey, J. Krall, and G. Joyce, *Phys. Rev. Lett.*, **69**, 2200 (1992).

[7] C. A. Coverdale, C. B. Darrow, C. D. Decker, W. B. Mori, K. -C. Tzeng, K. A. Marsh, C. E. Clayton, and C. Joshi, *Phys. Rev. Lett.* **74**, 4659, (1995).

[8] K. Nakajima, D. Fisher, T. Kawakubo, H. Nakanishi, A. Ogata, Y. Kato, Y. Kitagawa, R. Kodama, K. Mima, H. Shiraga, K. Suzuki, K. Yamakawa, T. Zhang, Y. Sakawa, T. Shoji, N. Yugami, M. Downer and T. Tajima, *Phys. Rev. Lett.* **74**, 4428, (1995).

[9] A. Modena, Z. Najmudin, A. E. Dangor, C. E. Clayton, K. A. Marsh, C. Joshi, V. Malka, C. B. Darrow, C. Danson, D. Neely and F. N. Walsh, *Letts. Nature* **377**, 606, (1995).

[10] D. Umstadter, S.-Y. Chen, A. Maksimchuk, G. Mourou, and R. Wagner, *Science* **273**, 472 (1996).

[11] A. Ting, K. Krushelnick, C. I. Moore, H. R. Burris, E. Esarey, J. Krall, and P. Sprangle, *Phys. Rev. Lett.* **77**, 5377 (1996).

[12] S. P. Le Blanc, M. C. Downer, R. Wagner, S.-Y. Chen, A. Maksimchuk, G. Mourou and D. Umstadter, *Phys. Rev. Lett.* **77**, 5381 (1996).

[13] R. Wagner, S.-Y. Chen, A. Maksimchuk and D. Umstadter, *Phys. Rev. Lett.* **78**, 3122 (1997).

[14] A. Chiron *et al.*, Phys. Plasmas **3**, 1373 (1996).

[15] C. Rousseaux, *et al.*, Phys. Fluids B, **4**, 2589 (1992).

[16] K.-C. Tzeng, *et al.*, *Advanced Accelerator Concepts 1996*, to be published.

[17] S. Humphries Jr., *Principles of Charged Particle Accelerators* (Wiley, New York, 1986).

[18] D. Umstadter, E. Esarey, and J. Kim, Phys. Rev. Lett. **72**, 1224 (1994); D. Umstadter *et al.*, Phys. Rev. E **51**, 3484 (1995).

[19] D. Umstadter, J. K. Kim, and E. Dodd, *Phys. Rev. Lett.* **76**, 2073 (1996).

[20] E. Esarey and M. Pilloff, Phys. Plasmas **2** 1432 (1995).

[21] See *e.g.*, *Advanced Accelerator Concepts, Fontana, WI, 1994*, Amer. Inst. of Conf. Proc. No. 335, P. Schoessow, ed., (AIP Press, New York, 1995) and references cited therein.